Supporting Information

Community transmission of SARS-CoV-2 by Surfaces: Risks and Risk Reduction Strategies

Ana K. Pitol[1] , Timothy R. Julian[2,3,4]

[1] Department of Civil and Environmental Engineering, Imperial College London, London SW7 2AZ, United Kingdom

[2]Eawag, Swiss Federal Institute of Aquatic Science and Technology, Dübendorf CH-8600, Switzerland

[3]Swiss Tropical and Public Health Institute, Basel CH-4051, Switzerland

[4]University of Basel, Basel CH-4055, Switzerland

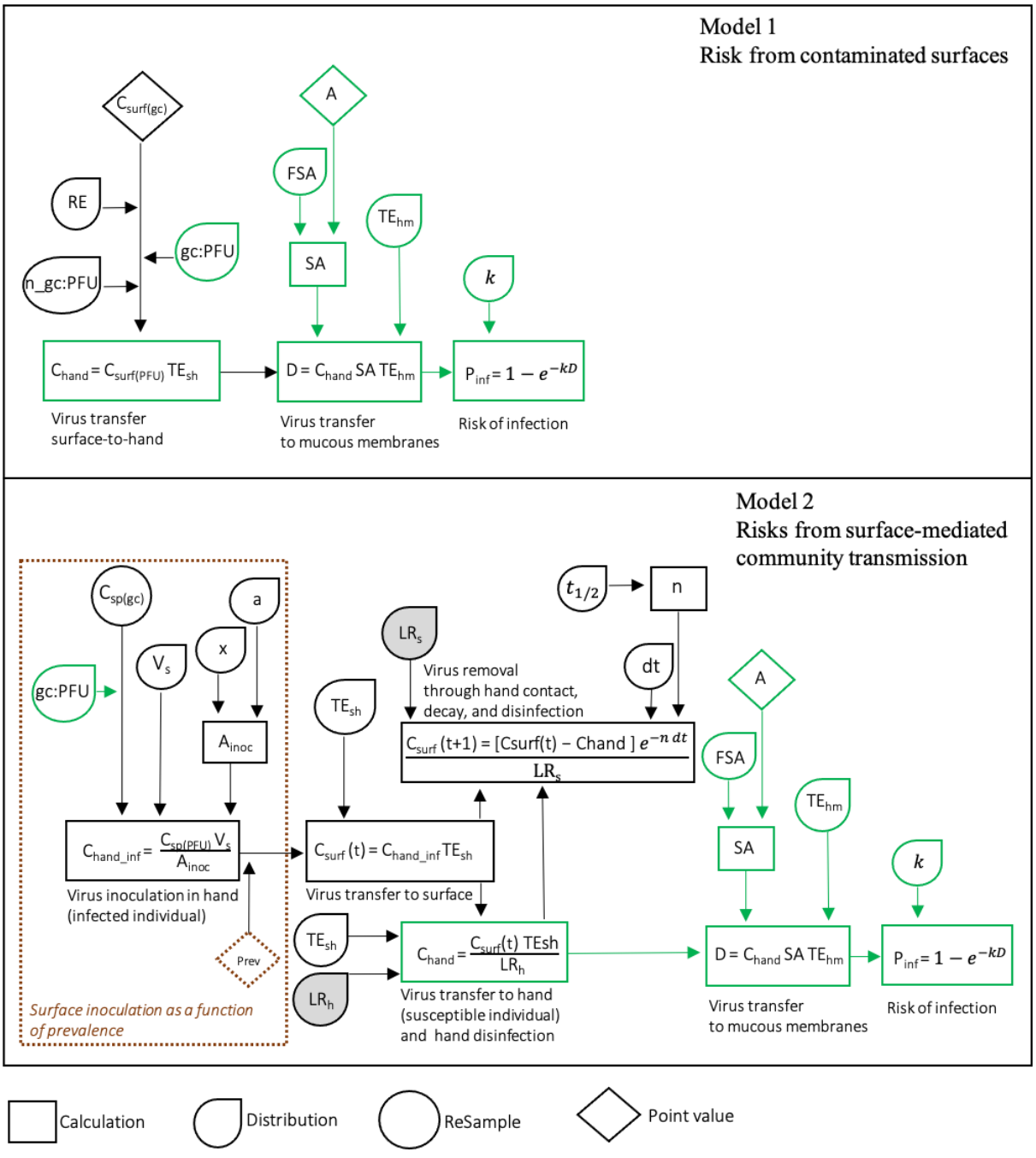

Figure S1. Diagram of the mathematical models used to estimate the risk from contaminated surfaces and the risk from surface-mediated community-transmission. Green rectangles represent shared equations or parameters between the risk model for contaminated surface and the risk model for surface-mediated community transmission. Within the dotted brown line we show the model used to calculate the surface contamination as a function of prevalence. Filled shapes represent the parameters only used in the intervention scenarios (log_{10} reduction values). The descriptions of parameters' and inputs can be found in Table 1.

Table S1. Input parameters for the risk assessment model

Parameter	Units	Description	Distributions (Input values)/ Equations	Reference and comments
$C_{sp\,(gc)}$	Gene copies (gc) mL^{-1}	Concentration of SARS-CoV-2 in sputum or saliva	ReSample (data set)	(1–4) RT-qPCR data on viral loads of 9, 2, 2, and 23 patients with COVID-19
$C_{surf\,(gc)}$	gc cm^{-2}	Concentration of SARS-CoV-2 in surfaces	Point values (102.4, 2.5, 11.6, 6.8, 1.2, 30, 39.3, 0.8, 0.8, 0.1)	(5, 6) RT-qPCR data on concentration of SARS-CoV-2 in surfaces found in public spaces
gc: PFU	unitless	Genome copies to infectious virus conversion factor. Used to convert the viral concentrations $C_{(gc)}$ to $C_{(PFU)}$	Uni (10^2-10^3)	(7, 8) Based on the ratio for influenza A(H1N1), A(H3N2), and influenza B and the ratio of $TCID_{50}$ to PFU
n_gc: PFU	unitless	Ratio of gc decay to infective virus decay on surfaces	Uni (1-50)	(9)Informed by data on the persistence of influenza on surfaces.
RE	unitless	Recovery efficiency	Point value (0.6)	(6) Recovery efficiency from swabs
V_s	mL	Volume of saliva expelled per cough	Uni (0.0396 - 0.0484)	(10) Volume of 0.044mL (11) Assumed uniform distribution using volume ± 10%
x	cm	Distance between hand and mouth	Uni (5-10)	Assumed
a	degrees	Right angle of cone	Uni (27.5-35)	Based on the images of people spreading particles while coughing(12, 13)
A_{inoc}	cm^2	Area of inoculation by cough	$A_{inoc} = \pi r^2$ $r = x\tan(a)$	(14) Calculated assuming viral particles spread conically (Supplementary Figure 1)
C_{hand_inf}	PFU cm^{-2}	Concentration of SARS-CoV-2 on the hands of an infected individual	$\frac{C_{sp} V_s}{A_{inoc}}$	(14) Calculated assuming viral particles spread conically (Supplementary Figure 1)
$t_{\frac{1}{2}stl}$	min	Half-life of SARS-CoV-2 in metal	N (338,35)	(15)Based on SARS-CoV-2 infectivity at 40% RH and 21-23°C
$t_{\frac{1}{2}pl}$	min	Half-life of SARS-CoV-2 in plastic	N (409,39)	(15)Based on SARS-CoV-2 infectivity at 40% RH and 21-23°C
n	min^{-1}	Exponential decay constant	$\frac{\ln 2}{t_{1/2}}$	Calculated assuming exponential decay
dt	min	Time between surface touching	Uni (1-20) Uni (60-240)	Based on public transport schedules in major cities Contact with surfaces was assumed to happen between 7 am and 11pm
TE_{hm}	%	Transfer efficiency from hand to mucous membranes	N (20,6.3)	(16)Transfer efficiency of viruses (MS2) from hand to saliva

TE_{sh_stl}	%	Transfer efficiency of virus between metal and hand	N (37.4, 16)	(17)Transfer efficiency of viruses (MS2) between steel and hand at 40-65% RH
TE_{sh_pl}	%	Transfer efficiency of virus between plastic and hand	N (79.5,21.2)	(17)Transfer efficiency of viruses (MS2) between plastic and hand at 40-65% RH
LR_s		Log_{10} reduction for surface disinfection	Uni (3-4)	(18, 19) Log_{10} reduction of coronaviruses on surfaces with ethanol and chlorine disinfection
LR_h		Log_{10} reduction for hand disinfection	Point value (4.25)	(20) Log_{10} reduction of SARS-CoV with alcohol-based (>75%) sanitizer
$Prev$	%	Prevalence	Point values Low (0.2%) Medium (1%) High (5%)	Medium prevalence based on rates encountered during the peak of the first wave of COVID-19 in major cities(21–25).
$C_{surf(t+1)}$	PFU cm^{-2}	Concentration of SARS-CoV-2 in surface at time = t+1	$\frac{(C_{surf(t)}-C_{hand})e^{-n\,dt}}{LR_h}$	Calculated
C_{hand}	PFU cm^{-2}	Concentration of SARS-CoV-2 on the hands of susceptible individuals	$\frac{C_{surf}\,TE_{sh}}{LR_h}$	Calculated
SA	cm^2	Surface area in contact with mucous membranes	Uni (3.9-5.9)	(26) Fractional surface area for partial finger. (27)Average hand surface area
D	PFU	Dose	$C_{hand}\,SA\;TE_{sh}$	Calculated
k	PFU^{-1}	Parameter of exponential dose-response	Tri (0.00107, 0.00246, 0.00680)	(28) Data obtained from QMRAwiki, based on 2 studies (29) (30) using the 0.5^{th}, 50^{th}, and 99.5^{th} percentiles as min, mode, and max
P_{inf}	unitless	Probability of infection	$1-e^{-kD}$	Calculated (28) Model obtained from QMRAwiki

Distributions and input parameters are abbreviated as follows: N= Normal (mean, SD), Uni =Uniform (min-max), Tri=Triangular (min, mode, max). ReSample refers to random sampling with replacement from the data set of of viral loads reported for patients with COVID-19 in the associated reference.

Inoculation of viruses on hands

We assumed that a cough spread particles conically(14) (Figure 1). The concentration of viruses (virus cm^{-2}) was estimated by calculating the surface area of a circle projected by the cone at a distance x from the mouth (Equations 1 and 2). Distance x was assumed to be a uniform distribution between 5 and 10 cm. The conical opening angle, between 27.5-35°, was informed by images of people spreading particles while coughing(12, 13).

$$r = x\tan(a) \qquad \text{(Equation 1)}$$

$$A_{inoc} = \pi r^2 \qquad \text{(Equation 2)}$$

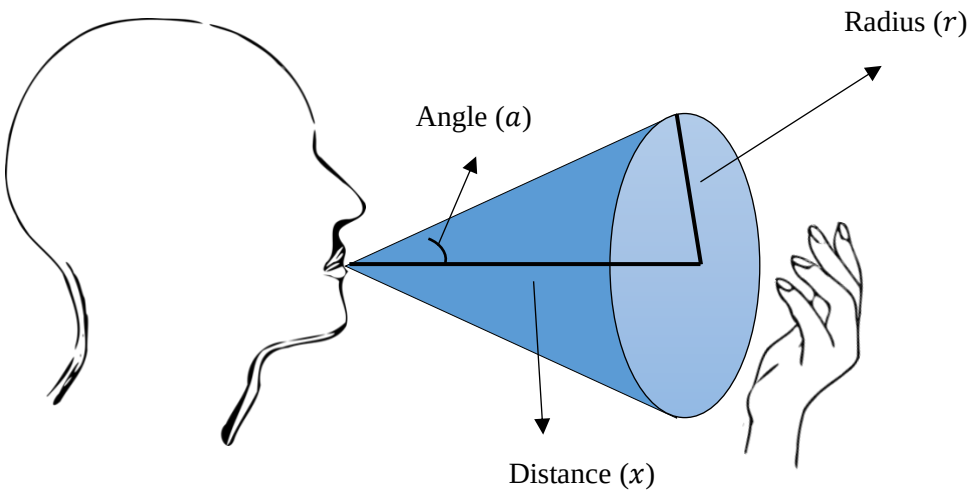

Figure S2. Conical distribution of particles through a cough

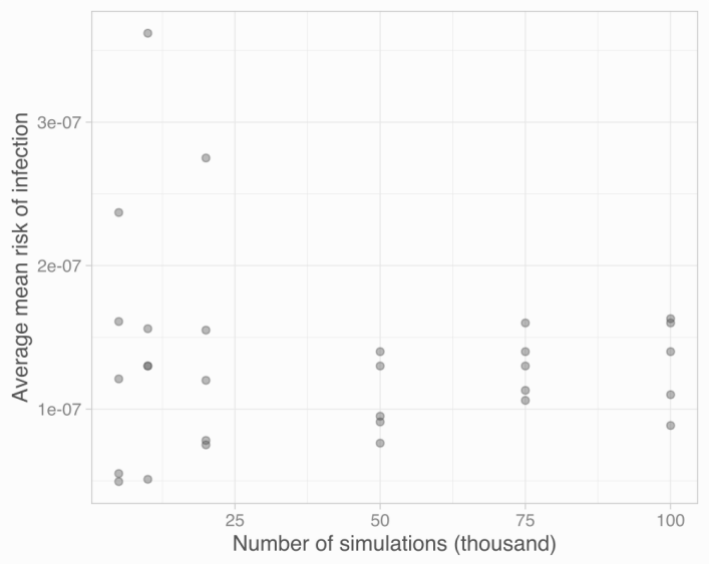

Figure S3. Risk of infection *vs* number of Monte Carlo simulations. The analyses were run five times for the baseline scenario (Prevalence 1%, no intervention) for 5000, 10000, 20000, 50000, 75000, and 100000 simulations. The average median risk of infection is shown in black circles.

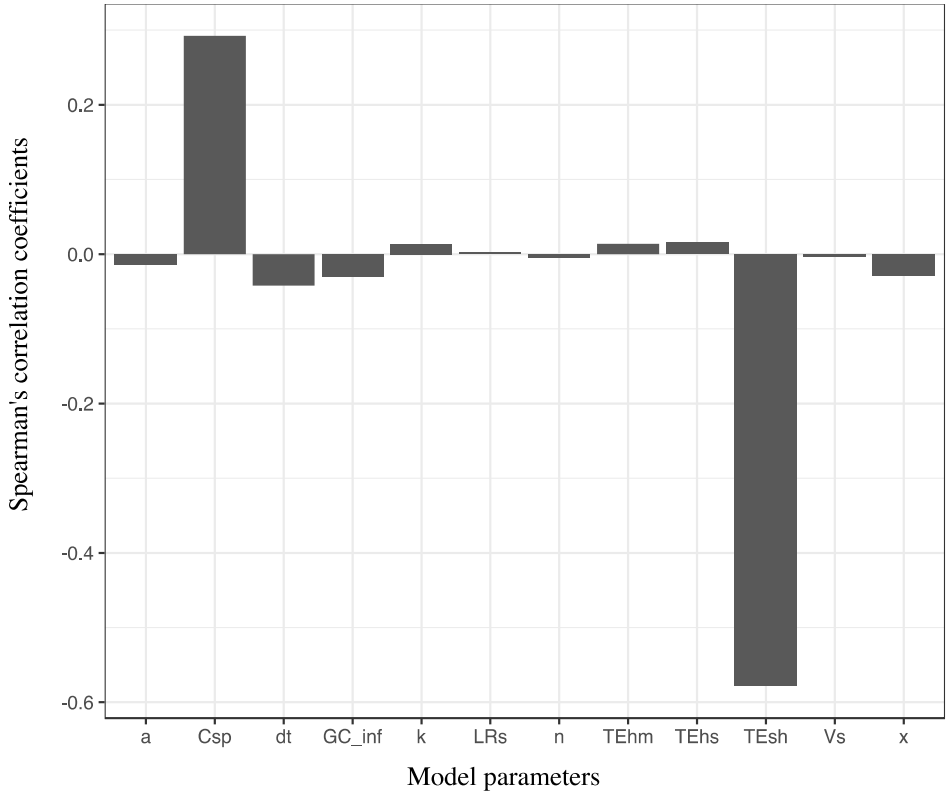

Figure S3. Sensitivity analysis for the "Risks from surface-mediated community transmission" model. Spearman's correlation coefficients for the parameters used in the community transmission model. Parameters are abbreviated as follows: a = opening angle of right cone, Csp = Concentration of SARS-CoV-2 in the sputum or saliva of patients, dt = contact frequency, GC_inf = genome copies(gc) per Plaque Forming Units (PFU) ratio, k = parameter of the dose-response exponential model, LRs = Log_{10} reduction due to surface disinfection, n = exponential decay constant, surf_dis = log_{10} reduction for surface disinfection, TEhm = transfer efficiency of viruses from hand to mouth, TEhs = transfer efficiency of viruses from hand to surface, TEsh = transfer efficiency of viruses from surface to hand, Vs = volume of saliva expelled per cough, x= distance between hand and mouth.

Table S2. Percentage of Contacts with Estimated Risks Above 10^{-4}

	Percentage of Contacts with Estimated Risks Above 1 in 10,000 (%)					
	Low Frequency Contacts			High Frequency Contacts		
	Low Prevalence	Medium Prevalence	High Prevalence	Low Prevalence	Medium Prevalence	High Prevalence
No Intervention	0.8	3.8	17.2	1.4	6.9	27.6
Hand Disinfection (compliance)						
25%	0.6	2.7	12.9	1.1	5.2	21.0
50%	0.4	1.9	9.3	0.8	3.4	14.8
75%	0.2	0.7	5.5	0.3	1.7	6.8
Surface Disinfection (times a day)						
Once (7am)	0.5	2.8	12.9	1.4	6.6	27.0
Once (12pm)	0.5	2.6	12.0	1.4	6.6	26.8
Twice (7am,12pm)	0.4	2.0	9.5	1.4	6.4	26.5

Low prevalence = 0.2% of the population was assumed to have the disease, medium prevalence = 1% of the population, and high Prevalence = 5% of the population.

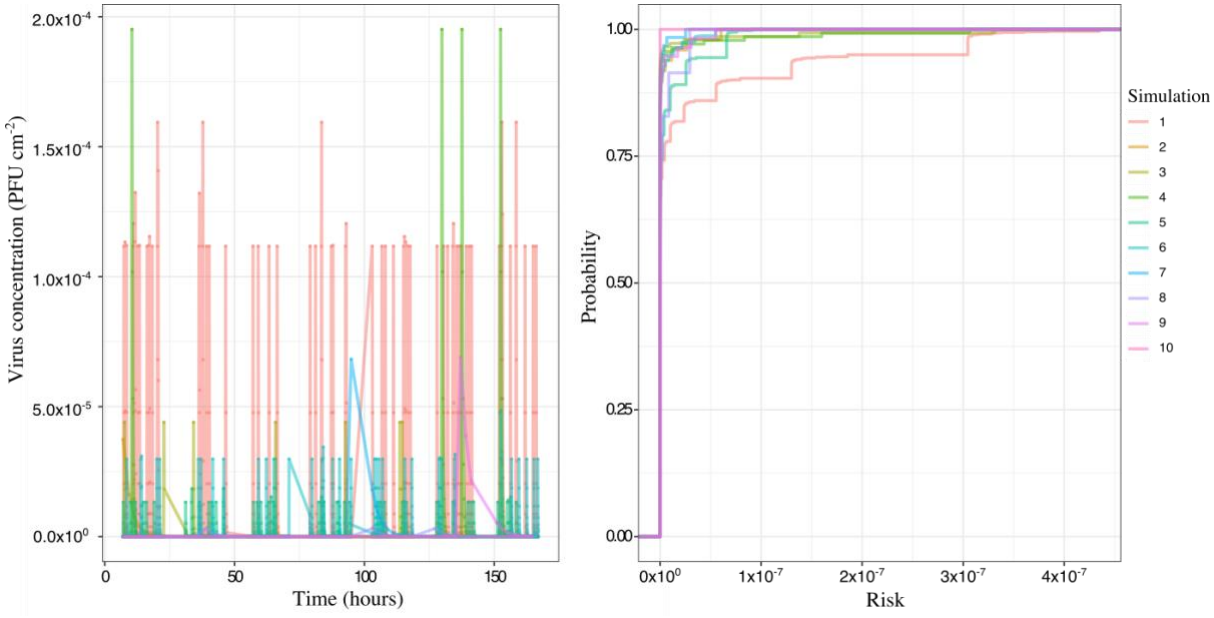

Figure S4. Modeled virus concentration across time for ten simulations (left), cumulative distribution function for risks for the same simulations (right). The community transmission model estimates concentrations across time for seven days (168 hours); inoculation of SARS-CoV-2 into the surface is considered to happen between 7 am and 11 pm.

References

1. Wölfel R, Corman VM, Guggemos W, Seilmaier M, Zange S, Müller MA, Niemeyer D, Jones TC, Vollmar P, Rothe C, Hoelscher M, Bleicker T, Brünink S, Schneider J, Ehmann R, Zwirglmaier K, Drosten C, Wendtner C. 2020. Virological assessment of hospitalized patients with COVID-2019. Nature 1–14.
2. Pan Y, Zhang D, Yang P, Poon LLM, Wang Q. 2020. Viral load of SARS-CoV-2 in clinical samples. Lancet Infect Dis 20:411–412.
3. Kim JY, Ko JH, Kim Y, Kim YJ, Kim JM, Chung YS, Kim HM, Han MG, Kim SY, Chin BS. 2020. Viral load kinetics of SARS-CoV-2 infection in first two patients in Korea. J Korean Med Sci 35:1–7.
4. To KKW, Tsang OTY, Leung WS, Tam AR, Wu TC, Lung DC, Yip CCY, Cai JP, Chan JMC, Chik TSH, Lau DPL, Choi CYC, Chen LL, Chan WM, Chan KH, Ip JD, Ng ACK, Poon RWS, Luo CT, Cheng VCC, Chan JFW, Hung IFN, Chen Z, Chen H, Yuen KY. 2020. Temporal profiles of viral load in posterior oropharyngeal saliva samples and serum antibody responses during infection by SARS-CoV-2: an observational cohort study. Lancet Infect Dis 20:565–574.
5. Abrahao JS, Pengo LS, Rezende IM, Rodrigues R, Crispim APC, Moura C, Mendonca DC, Reis E, Souza F, Oliveira GFG, Domingos IJ da S, Boratto P, e Silva PHB, Queiroz VF, Silva TB de S, Oliveira GP, Alves V de S, Alves PA, Kroon EG, Trindade G de S, Drumond BP. 2020. Detection of SARS-CoV-2 RNA on public surfaces in a densely populated urban area ofBrazil: A potential tool for monitoring the circulation of infected patients. Sci Total Environ.
6. Harvey A, Fuhrmeister E, Cantrell M, Pitol A, Swarthout J, Powers J, Julian T, Pickering A. 2020. Longitudinal monitoring of SARS-CoV-2 RNA on high-touch surfaces in a community setting. Environ Sci Technol Lett.
7. Ip DKM, Lau LLH, Chan KH, Fang VJ, Leung GM, Peiris MJS, Cowling BJ. 2015. The Dynamic Relationship between Clinical Symptomatology and Viral Shedding in Naturally Acquired Seasonal and Pandemic Influenza Virus Infections. Clin Infect Dis 62:431–437.
8. ATCC. 2012. Converting TCID50 to plaque forming units PFU-12. https://www.lgcstandards-

atcc.org/Global/FAQs/4/8/Converting_TCID50_to_plaque_forming_units_PFU-124.aspx?geo_country=gb (Accessed Sep 20, 2020)

9. Thompson KA, Bennett AM. 2017. Persistence of influenza on surfaces. J Hosp Infect 95:194–199.

10. Nicas M, Jones RM. 2009. Relative contributions of four exposure pathways to influenza infection risk. Risk Anal 29:1292–1303.

11. Adhikari U, Chabrelie A, Weir M, Boehnke K, McKenzie E, Ikner L, Wang M, Wang Q, Young K, Haas CN, Rose J, Mitchell J. 2019. A Case Study Evaluating the Risk of Infection from Middle Eastern Respiratory Syndrome Coronavirus (MERS-CoV) in a Hospital Setting Through Bioaerosols. Risk Anal 39:2608–2624.

12. Bandiera L, Pavar G, Pisetta G, Otomo S, Mangano E, Seckl JR, Digard P, Molinari E, Menolascina F, Viola IM. 2020. Face Coverings and Respiratory Tract Droplet Dispersion 1–15.

13. Bourouiba L, Dehandschoewercker E, Bush JWM. 2014. Violent expiratory events: On coughing and sneezing. J Fluid Mech 745:537–563.

14. Nicas M, Sun G. 2006. An integrated model of infection risk in a health-care environment. Risk Anal 26:1085–1096.

15. van Doremalen N, Bushmaker T, Morris DH, Holbrook MG, Gamble A, Williamson BN, Tamin A, Harcourt JL, Thornburg NJ, Gerber SI, Lloyd-Smith JO, de Wit E, Munster VJ. 2020. Aerosol and Surface Stability of SARS-CoV-2 as Compared with SARS-CoV-1. N Engl J Med.

16. Pitol AK, Bischel H, Kohn T, Julian TR. 2017. Virus transfer at the skin-liquid interface. Environ Sci Technol 51:14417–14425.

17. Lopez GU, Gerba CP, Tamimi AH, Kitajima M, Maxwell SL, Rose JB. 2013. Transfer efficiency of bacteria and viruses from porous and nonporous fomites to fingers under different relative humidity conditions. Appl Environ Microbiol 79:5728–5734.

18. Hulkower RL, Casanova LM, Rutala WA, Weber DJ, Sobsey MD. 2011. Inactivation of surrogate coronaviruses on hard surfaces by health care germicides. Am J Infect Control

39:401–407.

19. Sattar SA, Springthorpe VS, Karim Y, Loro P. 1989. Chemical disinfection of non-porous inanimate surfaces experimentally contaminated with four human pathogenic viruses. Epidemiol Infect 102:493–505.

20. Rabenau HF, Kampf G, Cinatl J, Doerr HW. 2005. Efficacy of various disinfectants against SARS coronavirus. J Hosp Infect 61:107–111.

21. Bendavid E, Mulaney B, Sood N, Shah S, Ling E, Bromley-Dulfano R, Lai C, Weissberg Z, Saavedra R, Tedrow J, Tversky D, Bogan A, Kupiec T, Eichner D, Gupta R, Ioannidis J, Bhattacharya J. 2020. COVID-19 Antibody Seroprevalence in Santa Clara County, California. medRxiv 2020.04.14.20062463. (Accessed Oct 10, 2020)

22. Perez-Saez J, Lauer SA, Kaiser L, Regard S, Delaporte E, Guessous I, Stringhini S, Azman AS. 2020. Serology-informed estimates of SARS-CoV-2 infection fatality risk in Geneva, Switzerland. Lancet Infect Dis 3099:2–3.

23. Pollán M, Pérez-Gómez B, Pastor-Barriuso R, Oteo J, Hernán MA, Pérez-Olmeda M, Sanmartín JL, Fernández-García A, Cruz I, Fernández de Larrea N, Molina M, Rodríguez-Cabrera F, Martín M, Merino-Amador P, León Paniagua J, Muñoz-Montalvo JF, Blanco F, Yotti R. 2020. Prevalence of SARS-CoV-2 in Spain (ENE-COVID): a nationwide, population-based seroepidemiological study. Lancet 6736:1–11.

24. Erikstrup C, Hother CE, Pedersen OBV, Mølbak K, Skov RL, Holm DK, Sækmose SG, Nilsson AC, Brooks PT, Boldsen JK, Mikkelsen C, Gybel-Brask M, Sørensen E, Dinh KM, Mikkelsen S, Møller BK, Haunstrup T, Harritshøj L, Jensen BA, Hjalgrim H, Lillevang ST, Ullum H. 2020. Estimation of SARS-CoV-2 infection fatality rate by real-time antibody screening of blood donors. Clin Infect Dis.

25. Amorim Filho L, Szwarcwald CL, Mateos S de OG, Leon ACMP de, Medronho R de A, Veloso VG, Lopes JIF, Porto LC de MS, Chieppe A, Werneck GL, Grupo Hemorio de Pesquisa em Covid-19. 2020. Seroprevalence of anti-SARS-CoV-2 among blood donors in Rio de Janeiro, Brazil. Rev Saude Publica 54:69.

26. AuYeung W, Canales RA, Leckie JO. 2008. The fraction of total hand surface area involved in

young children's outdoor hand-to-object contacts. Environ Res 108:294–299.

27. US Environmental Protection Agency. 2011. Exposure Factors Handbook: 2011 Edition. US Environ Prot Agency 1:1–1466.

28. Haas C. WikiQMRA: Completed Dose Response Models. http://qmrawiki.org/framework/dose-response/experiments (Accessed Aug 2, 2020).

29. De Albuquerque N, Baig E, Ma X, Zhang J, He W, Rowe A, Habal M, Liu M, Shalev I, Downey GP, Gorczynski R, Butany J, Leibowitz J, Weiss SR, McGilvray ID, Phillips MJ, Fish EN, Levy GA. 2006. MurineHepatitis Virus Strain 1 Produces a Clinically Relevant Model of Severe Acute Respiratory Syndrome in A/J Mice. J Virol.

30. DeDiego ML, Pewe L, Alvarez E, Rejas MT, Perlman S, Enjuanes L. 2008. Pathogenicity of severe acute respiratory coronavirus deletion mutants in hACE-2 transgenic mice. Virology.